Science of the Total Environment 894 (2023) 165093

Contents lists available at ScienceDirect

Science of the Total Environment

journal homepage: www.elsevier.com/locate/scitotenv

Urbanization as a limiter and catalyst of watershed-scale sediment transport: Insights from probabilistic connectivity modeling

Isaac McVey [a], Alexander Michalek [b], Tyler Mahoney [c], Admin Husic [a,*]

[a] Dept. of Civil, Environmental and Architectural Engineering, University of Kansas, United States of America
[b] Dept. of Civil and Environmental Engineering, University of Iowa, United States of America
[c] Dept. of Civil and Environmental Engineering, University of Louisville, United States of America

HIGHLIGHTS

- Urbanization decreases the maximal spatial extent of watershed-scale connectivity.
- Urbanization focuses sediment transport into fewer, frequently wetted pathways.
- Watershed-scale connectivity corresponds to stream sediment loading 50 % of the time.

GRAPHICAL ABSTRACT

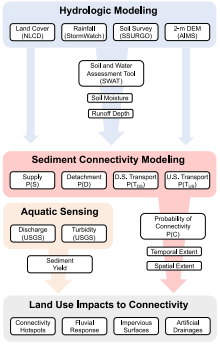

ARTICLE INFO

Editor: Fernando A.L. Pacheco

Keywords:
Urbanization
Sediment
Connectivity
Probability
Numerical modeling

ABSTRACT

The conversion of rural lands to urban areas exerts considerable influence on the hydrologic processes governing sediment transport at the watershed scale. While the effects of urbanization on hydrology have been well-studied, the corresponding impact to the spatial and temporal variability of sediment detachment, transport, and connectivity is less certain. To address this knowledge gap, we apply process-based hydrologic simulation, probabilistic connectivity modeling, and in situ turbidity sensing to five watersheds positioned along a steep land use gradient in Kansas, USA. Connectivity modeling results show that urbanization systematically decreases the maximal extent of watershed-scale connectivity on the wettest days of the study period, from 51 % in the most rural watershed to 28 % in the most urban watershed. On the other hand, urbanization focuses sediment transport into fewer, more frequently wetted pathways, such as roadway drainage networks, which are activated 3.5 times more frequently than the equivalent pathways in rural basins. In this way, urbanization limits maximal connectivity as impervious surfaces indefinitely disconnect source zones from the sediment cascade, but also catalyzes hot spots of connectivity as these same impervious areas generate excess runoff and channel it to drainage systems. The 23.9 ± 4.2 % of days that exhibit watershed-scale functional connectivity account for 85.0 ± 9.5 % of sediment export with most of the export tied to a few highly connected days. Sensing results show that increases in watershed-scale connectivity only translate to larger fluvial sediment loads after a connectivity threshold (the median connected day) has been exceeded, suggesting a transition from functional to structural connectivity control on sediment dynamics after sufficient wetting. This study highlights the role of land use impacts on the sources and mechanisms of sediment transport, which will be an important consideration for land managers as urban areas continue to expand to accommodate global migration patterns.

* Corresponding author at: 2134B Learned Hall, University of Kansas, Lawrence, KS 66045, United States of America.
E-mail address: ahusic@ku.edu (A. Husic).

http://dx.doi.org/10.1016/j.scitotenv.2023.165093
Received 19 April 2023; Received in revised form 14 June 2023; Accepted 21 June 2023
Available online 22 June 2023

1. Introduction

Managing soil erosion is one of the largest sustainability challenges of the 21st century (Borrelli et al., 2020). Land use change, such as urbanization and agricultural exploitation, often exacerbates soil erosion and can cause reduced agricultural productivity, stream degradation, aquatic habitat loss, and infrastructure risk (Wood and Armitage, 1997; Russell et al., 2018; Llena et al., 2019; Kroese et al., 2020). Soil erosion will continue to be an ongoing environmental concern as the global urban population is projected to nearly double to 66 % of the world's population by 2050 (Bettencourt et al., 2018; Borrelli et al., 2020). In urban regions, widespread impervious land cover acts to induce greater runoff and shear, which increase the capacity for sediment transport (Ferreira et al., 2020; Noe et al., 2020). In rural areas, removal of native vegetation and tilling practices expose bare sediment and increase the supply for potential transport (Kroese et al., 2020). How sediment is linked from source to sink, termed connectivity, has been the topic of much recent study (Fryirs et al., 2007; Borselli et al., 2008; Bracken et al., 2015; Mahoney et al., 2018, 2020a, 2020b); however, there exists a lack of studies that address the role of land use impacts in shifting the dominant sources, transport pathways, and mechanisms of sediment connectivity.

Sediment connectivity is the transfer of eroded sediment between landscape components and is a function of static and dynamic watershed attributes (Fryirs et al., 2007), giving rise to two forms of sediment connectivity: structural and functional (Heckmann et al., 2018; Baartman et al., 2020; Michalek et al., 2021). Structural connectivity refers the spatial configuration of morphometric features within a system, such as slope and soil texture, that vary little from one event to the next. On the other hand, functional connectivity refers to the dynamic variability through space and time of runoff and soil moisture conditions in response to hydrologic events. Models and concepts of these two connectivity paradigms have emerged, such as the Index of Connectivity (IC; Borselli et al., 2008), which estimates structural connectivity, and the Probability of Sediment Connectivity (P(C); Mahoney et al., 2018), which estimates structural and functional connectivity. The IC approach has been successfully applied to investigate land use impacts (Michalek et al., 2021), landslide susceptibility (Persichillo et al., 2018), and continental-scale climatic and tectonic drivers (Husic and Michalek, 2022). A major advantage of IC is that it has few data requirements, can be calculated from remotely sensed products, and modeling packages exist for rapid assessment (Crema and Cavalli, 2018; Baldan et al., 2022). However, a limitation of IC is that it does not consider the dynamic nature of runoff and soil moisture conditions that may vary considerably over the course of a hydrologic event. Functional connectivity models, such as P(C), overcome these limitations by resolving runoff and soil moisture through process-based modeling (Bracken et al., 2015; Mahoney et al., 2018). There is potential for these dynamic models to inform how land use change alters connectivity processes related to the supply, detachment, and transport of sediment from source to sink.

Dynamic connectivity modeling requires the determination of hydrologic processes, such as runoff and soil moisture, which can be achieved with process-based models like the Soil Water Assessment Tool (SWAT) (Arnold et al., 1998). These models simulate the wetting of the landscape and the movement of water from the uplands to rivers, which are crucial components of connectivity modeling (Mahoney et al., 2018). The watershed-scale probabilistic connectivity approach uses these outputs from the hydrologic model together with sediment supply, detachment, and transport estimates to infer connected zones within a watershed (Mahoney et al., 2020b). Where sediment is available, easily detachable, and transport pathways exist, watershed-scale connectivity is expected to prevail, such as in the case of roadside ditches that are designed to efficiently convey flow. Conversely, where these processes are inhibited or not present, such as in the case of impervious surfaces disconnecting supply zones, then connectivity may be limited as a result. However, the potential for connectivity in the uplands of a watershed does not necessarily translate to pulses of sediment delivery to the stream corridor, due to the presence of disconnectivities (Fryirs, 2013). To that end, in situ sensing of fluvial turbidity (a proxy for sediment concentration) together with numerical modeling can allow for identification of when a watershed meaningfully contributes sediment to a river system (Zarnaghsh and Husic, 2021). While hydrologic modeling, connectivity estimation, and aquatic sensing have individually (or in tandem) informed investigation of sediment processes, there is a need to integrate these approaches to assess the impact of urbanization on the sediment linkage, from the uplands to the river network.

The objective of this study was to assess the impact of urbanization on dynamic sediment connectivity at the watershed-scale. We hypothesized that urban watersheds experience greater sediment connectivity due to increased runoff and excess shear generated from impervious surfaces. To test this hypothesis, we calibrated a process-based hydrologic model of soil moisture and runoff processes, applied a probabilistic connectivity model of erosion and transport processes, and compared in situ turbidity sensing data to hydrologic and sediment connectivity model predictions. Thereafter, we investigate the primary land use features, such as roadway drainages and agricultural fields, that have the potential to influence watershed-scale connectivity. Lastly, the conceptual model and results presented herein can be used to inform the prioritization of highly connected, erosion-prone hotspots for remediation and management.

2. Study site and materials

2.1. Study site

Johnson County is an urbanizing region in northeastern Kansas that has experienced a 33 % growth in population in the last two decades compared to 4 % growth for the rest of Kansas (USCB, 2020). To facilitate the rapid expansion in population growth, land use in the county has shifted from agriculture to urban (Fig. 1). The geographical region is categorized as lowland plains with an average slope of 3.7° and a temperate climate (mean annual rainfall: 958 mm). The soils in the study site are primarily silt loam and silt clay loam (Percich et al., 2022). In the present study, the five largest watersheds in Johnson County are considered: Blue River, Kill Creek, Cedar Creek, Mill Creek, and Indian Creek (Table S1). The watersheds have similar characteristics such as drainage area, precipitation, and topography but differ greatly with regard to the extent of urban land use and impervious surface cover. Indian Creek (91.7 %) and Mill Creek (65.4 %) are the most urbanized basins while Cedar Creek (34.7 %), Kill Creek (26.2 %), and Blue River (21.5 %) less so. As land cover is the definitive feature that alters hydrologic processes and sediment transport across the five watersheds, this study region provides an excellent testbed to examine the impact of urbanization on watershed-scale sediment connectivity.

2.2. Materials

Each of the study watersheds was instrumented with a stream gage and high-frequency turbidity sensor by the United States Geological Survey (Rasmussen and Gatotho, 2014), including Blue River (068931000), Kill Creek (06892360), Cedar Creek (06892495), Mill Creek (06892513), and Indian Creek (06893390) (USGS, 2018). Continuous estimates of sediment concentration were inferred from turbidity sensing data through linear regression to field-collected suspended sediment samples (n = 18 to 30; R^2 = 0.80 to 0.93; Rasmussen and Gatotho, 2014). The data from these sites were used to calibrate the hydrologic model and assess storm-driven delivery of sediment to river corridors. Daily meteorological forcing data, such as precipitation, relative humidity, wind speed, and temperature were retrieved from eleven weather stations in Johnson County (Storm Watch, 2020). Other forcing data like solar radiation were retrieved from Data Access MERRA-2 (Sparks, 2018). Landcover datasets for land use and soil composition were downloaded from National Land Class Database (Wickham et al., 2021; NLCD, 2004; NLCD, 2006) and the National Cooperative Soil Survey (USDA, 2021), respectively. Road networks were retrieved from the topologically integrated geographic encoding and

referencing (TIGER) data set (USCB, 2007). To resolve fine-scale topographic changes, high resolution 2-m digital elevation maps (DEMS) were provided by Johnson Country Automated Information Mapping Systems (AIMS, 2020).

3. Methods

To assess the impact of land use on sediment connectivity, we developed a workflow that incorporates (1) hydrologic modeling, (2) sediment connectivity modeling, and (3) aquatic sensing (Fig. 2). Hydrologic modeling is critical to assessing soil moisture conditions and the generation of runoff, which serve as the mechanisms for entraining particles into the sediment cascade in low-relief watersheds. Sediment connectivity modeling provides a probabilistic assessment of the likelihood for the landscape to have erodible sediment that can be detached and transported to a downstream sink. Lastly, aquatic sensing is used to assess the delivery of pulses of sediment to the stream corridor as a result of hydrologically driven flow path activation. Together, these approaches will aid in identifying connectivity hotspots and the fluvial response to rainfall as well as elucidating the impact of impervious surfaces and artificial drainages on sediment connectivity.

3.1. Runoff and soil moisture modeling

3.1.1. Soil water assessment tool

Hydrologic modeling was performed using the Soil Water Assessment Tool (SWAT). SWAT is a continuous, lumped parameter, process-based model used to simulate the input, storage, routing, and discharge of water within a watershed (Arnold et al., 2012; Zhang et al., 2019). SWAT accepts meteorological forcing data as inputs, solves internal mass-balances following parameterization laws, and outputs state and flux variables such as soil moisture, runoff, and discharge. Geospatial data inputs include land cover data, soil data, topology, and watershed routing information, which aid in parameterizing the discretized model subdomains. SWAT discretizes the basin of interest into several Hydrologic Response Units (HRUs), which are groupings of areas with similar land use, soil type, and slope. For each HRU, SWAT generates outputs that include soil moisture, runoff, ground water evaporation, daily curve number, among many other variables. These outputs are generated for a simulation time step prescribed by the modeler, which in the present case is daily. For our study basins, there were over 1200 unique HRUs identified by SWAT, but for computational purposes, less-common HRUs were grouped together down to the 500 most common HRUs. These 500 most common HRUs represent >90 % of the landscape, thus we are confident that the HRU selection captures the spatial variability in the basin, particularly considering that most SWAT studies do not exceed 400 HRUs (Wellen et al., 2015).

The basic mass balance equation that SWAT computes to simulate the hydrologic cycle is the soil water content:

$$SW_t = SW_0 + \Sigma_{i=1}^{t}\left(R_{day} - Q_{surf} - E_a - w_{seep} - Q_{gw}\right) \quad (1)$$

where SW_t is final soil water content on day i (mm), SW_0 is the initial soil water content (mm), R_{day} is the precipitation (mm), Q_{surf} is the surface runoff (mm), E_a is the amount of evapotranspiration (mm), w_{seep} is the amount of lateral flow or the amount of water entering the vadose zone (mm), and Q_{gw} is the amount of return flow to a stream (mm). Daily runoff for the HRUs (Q_{surf}) was determined with NRCS equation as:

$$Q_{surf} = \frac{\left(R_{day} - I_a\right)^2}{\left(R_{day} - I_a + S\right)^2} \quad (2)$$

where I_a represents the initial soil abstractions, such as interception, and soil infiltration prior to day i (mm) and S is the soil retention parameter (mm) (NRCS, 1972). The retention parameter (S) varies spatially with changes in soil, land cover, and slope, and temporally with changes in soil water content. The parameter can be calculated as

$$S = 25.4\left(\frac{1000}{CN} - 10\right) \quad (3)$$

where CN is the curve number for any given day. The Probability of Connectivity model requires daily runoff (Q_{surf}) and daily curve number (CN) estimates, thus these variables are of particular interest as the model was calibrated and validated in the following steps.

3.1.2. Calibration, validation, and uncertainty

A semi-automated Calibration Uncertainty Program (SWAT-CUP) was used to find optimal parameterizations for the hydrologic model. Within SWAT-CUP, the Sequential Uncertainty Fitting (SUFI-2) algorithm was applied to calibrate, validate, and perform sensitivity analysis (Abbaspour et al., 2007). We used a survey of literature values or the SWAT defaults to set the range of all model parameters (Table S2 and S3). The distribution of values for each parameter was assumed to be uniform and Latin hypercube sampling was conducted to assess uncertainty. Lastly, the 95 % prediction uncertainty (95 PPU) was determined by the 2.5 % and 97.5 % levels of cumulative distribution obtained from the uncertainty analysis (Abbaspour, 2015).

The SWAT models were calibrated and validated to average daily flow data at each watershed's outlet from January 1st, 2004 to December 31st, 2007. Three years (2001 to 2004) were used for model warm up, two years were used for calibration (2004 to 2005), and two years were used for validation (2006 to 2007). These modeling time periods were chosen to coincide with the availability of high frequency turbidity sensing data at our sites. The objective functions we used for calibrating the models were the Nash-Sutcliffe Efficiency (NSE) and the modified Kling Gupta Efficiency (KGE') due to their prominence in the hydrologic modeling literature (Clark et al., 2021; Ferreira et al., 2020). The equations for these metrics can be found in the Supplementary Materials. NSE is bound by negative infinity and 1 with the upper bound implying a perfect relationship between the simulated and observed discharge. Larger values of KGE' reflect better model performance with a value of 1 indicating a perfect match to observed data. The recommended NSE value for 'satisfactory' hydrologic model is approximately 0.50 for a daily time-step (Moriasi et al., 2015). Exact benchmarks for 'satisfactory' model performance using KGE are not well-established, but recent work relates a KGE of −0.41 to an NSE of 0 (the score associated with using the mean of the time series to predict the model; Knoben et al., 2019), thus we aim for our models to far exceed that threshold. Additionally, two other metrics were used to assess the 95 PPU: the p-factor and r-factor. The p-factor is the percentage of observed data that fits within the 95 PPU and r-factor is the thickness of the 95 PPU band envelop (Arnold et al., 2012; Abbaspour, 2015). Ideally, the p-factor should be close to 1 and the r-factor should be close to 0.

3.2. Dynamic connectivity modeling

3.2.1. Probability of connectivity

Dynamic sediment connectivity modeling aims to predict the likelihood that sediment eroded at its source is connected to a stream network during a storm event (Mahoney et al., 2018). First, the dynamic connectivity model approach requires distributed soil moisture and runoff estimates as inputs, which we continuously simulate using the calibrated SWAT model. Second, sediment connectivity can be modeled using a probabilistic approach to approximate areas that impact transport of sediment from upland source to the stream network (Mahoney et al., 2018). This probabilistic estimate is termed the probability of sediment connectivity, P(C), which is mathematically formulated as the intersection of multiple probabilities, which represent processes leading to sediment transport:

$$P(C) = P(S) \cap P(D_H \cup D_{NH}) \cap P(T_H \cup T_{NH}) \cap \{1 - P(B)\} \quad (6)$$

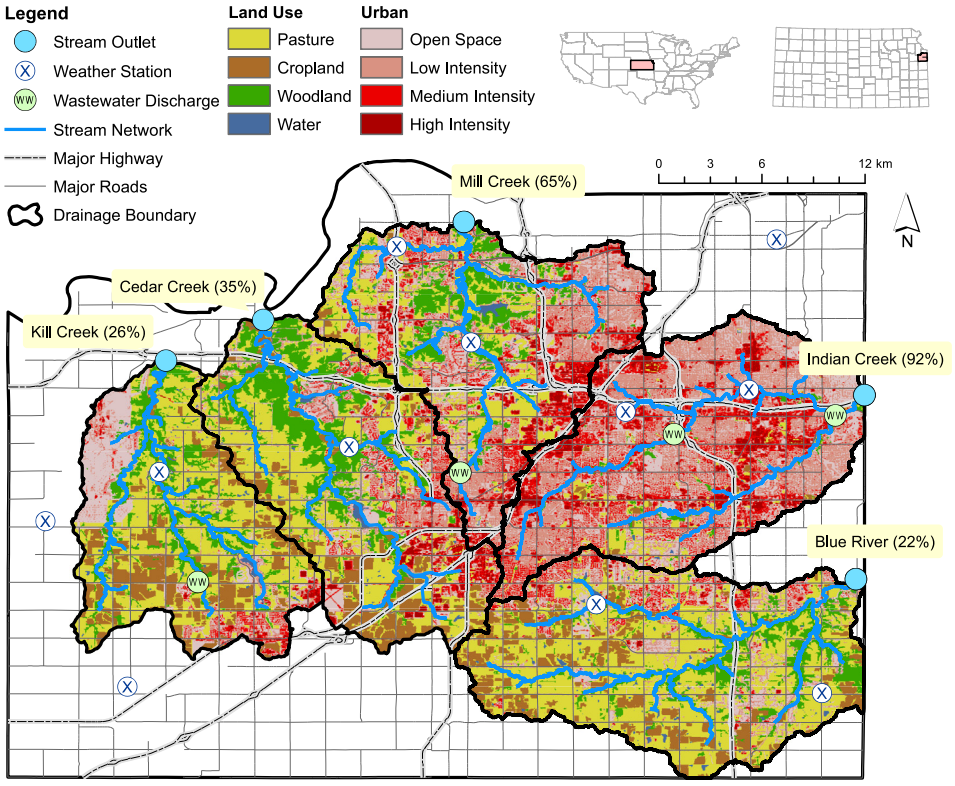

Fig. 1. Map of stream monitoring sites, weather stations, wastewater treatment facilities, major and minor roads, stream networks, and land use of the study watersheds within Johnson County, Kansas, USA. The percent urban land cover for each watershed is indicated in the title of each stream outlet.

where P(S) denotes the probability of sediment supply, $P(D_H)$ is probability of hydrologic detachment, $P(D_{NH})$ is probability of non-hydrologic detachment, $P(T_H)$ is probability of hydrologic transport, $P(T_{NH})$ is probability of non-hydrologic transport, and P(B) is probability of sediment buffers. The intersections and unions in Eq. (6) can be expanded to:

$$P(C) = P(S)[P(D_H) + P(D_{NH}) - P(D_H)P(D_{NH})] \times [P(T_H) + P(T_{NH}) - P(T_H)P(T_{NH})]\{1 - P(B)\} \quad (7)$$

Each probability in Eq. (7) can be calculated when a process is either known or can be estimated. Except for P(S), all other probability terms are simulated with a Boolean approach whereby each modeled probability for each geospatial grid cell is either a "0" or "1". For example, regarding detachment, a grid cell may either have sufficient runoff to exceed the critical shear stress, $P(D_H) = 1$, or not, $P(D_H) = 0$. A complete treatment of the terms, background, and justification for Eq. (7) can be found in Mahoney et al. (2018). Below, we will simplify Eq. (7) to consider assumptions and characteristics specific to our study area. First, non-hydrologic detachment $P(D_{NH})$ or non-hydrologic transport $P(T_{NH})$ was not considered as most transport occurs via modeled hydrologic processes as opposed to mass wasting events, such as landslides. Second, we do not consider the probability of buffers P(B). Mahoney et al. (2018) parameterized the potential impact of buffers P(B) with a field survey of their 65 km^2 basin. Our study area spans a drainage of >600 km^2, precluding the feasibility of a field survey. In their study, buffers contributed the least to disconnectivity of all factors (Mahoney et al., 2018), thus there is confidence that our results will remain accurate without the inclusion of P(B). Nonetheless, this is a potential limitation that will be discussed later. Considering these assumptions, Eq. (7) simplifies to the intersection of the remaining probabilities as $P(C) = P(S) \cap P(D) \cap P(T)$. This simplified equation is solved for every grid cell in the model domain for each day in the simulation period. Thereafter, the results for all grids are integrated over each watershed's spatial extent to get an overall assessment of watershed-scale connectivity for each day.

To determine the probability of sediment supply, P(S), we consider the percent impervious area within a cell (30-m by 30-m grid) to determine the extent to which sediment is disconnected. The following equation was used to simulate P(S) for each geospatial cell (i) as:

$$P_i(S) = \begin{cases} 1 - f_{imperv}, \text{if sediment is present in the cell} \\ 0, \text{if sediment is absent from the cell} \end{cases} \quad (8)$$

where *i* is the index for the geospatial cell and f_{imperv} is the fraction of impervious land cover. Fraction impervious surface was extracted at each grid from aerial imagery contained in the National Land Cover Data (NLCD, 2004). These results were resampled to 2-m by 2-m resolution to match the topographic DEM resolution used in the hydrologic modeling.

To determine the probability of detachment P(D), the excessive fluid shear stress principle was used as:

$$P_{i,j}(D) = \begin{cases} 1, \text{if } \tau_{f\,i,j} - \tau_{cr\,i} > 0 \\ 0, \text{if } \tau_{f\,i,j} - \tau_{cr\,i} \le 0 \end{cases} \quad (9)$$

where *j* is the index for the time step, $\tau_{f\,i,j}$ is the fluid shear stress of runoff ($N\,m^{-2}$), and $\tau_{cr\,i}$ is the critical shear stress ($N\,m^{-2}$). P(D) varies temporally due to changes in runoff depth as a function of precipitation and soil conditions. The fluid shear stress was approximated with the fluid momentum equation, considering one dimensional flow as:

$$\tau_f = \gamma R_{i,j} S_i \quad (10)$$

where γ is the specific weight of water ($N\,m^{-3}$), $R_{i,j}$ is the runoff depth determined from the hydrologic model (mm), and S_i is the slope of the

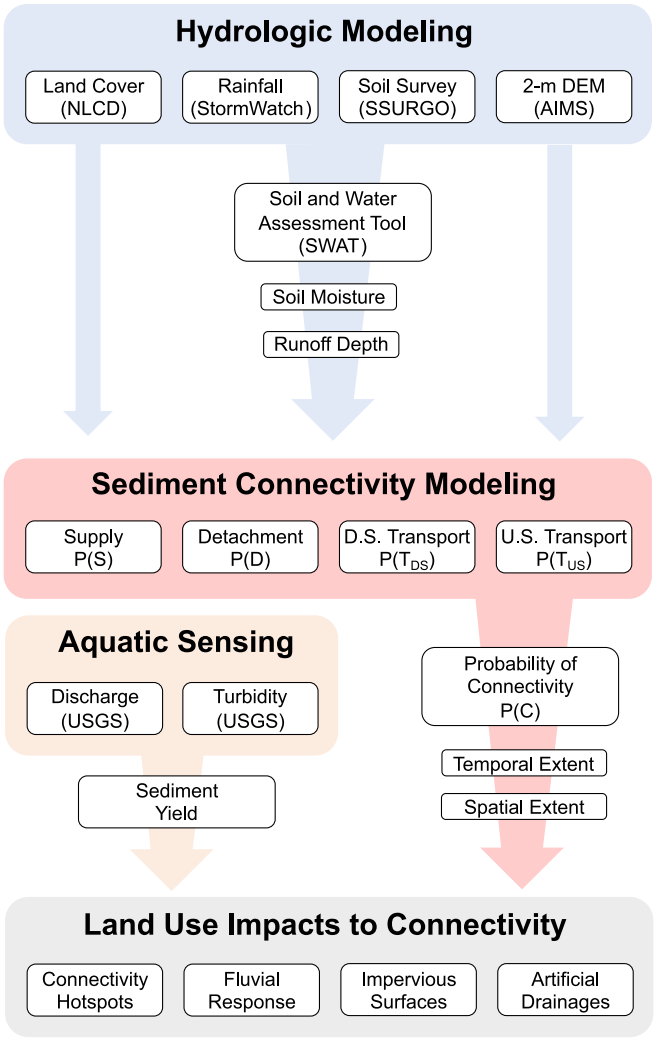

Fig. 2. Framework for integrating hydrologic modeling, sediment connectivity modeling, and aquatic sensing to assess land use impacts on watershed-scale dynamic sediment connectivity.

geospatial cell (m/m). Critical shear stress was predicted using the empirical critical shear stress equation for rangeland soil (Alberts et al., 1995), which considers sand fraction, organic matter content, and bulk sand density. The data for soil characteristics were available as soil geospatial layers using Soil Data Viewer (USDA, 2021).

The probability of upstream transport $P(T_{US})$ was parameterized by the notion that upstream drainage area may be a proxy for volume of concentrated runoff with enough magnitude and duration to sustain erosion (Vandaele, 1993) as:

$$P_i(T_{US}) = \begin{cases} 1, \text{if } S_i - S_{cr} > 0 \\ 0, \text{if } S_i - S_{cr} \le 0 \end{cases} \quad (11)$$

where S_{cr} is the critical slope required to initiate gully incision within in geospatial cell (m/m). Critical slope was parameterized using the formulations by Vandaele (1993) and Torri and Poesen (2014), which consider curve number, rock cover fragment, and organic matter content as well as the sand, silt, and clay fractions. The necessary characteristics are retrieved as soil geospatial layers using Soil Data Viewer (USDA, 2022). The daily curve number for each HRU is output by the SWAT model and it aims to simulate the effect that soil moisture, vegetation, land use, and soil type have on runoff abstractions.

Finally, the probability of downstream transport $P(T_{DS})$ was parameterized by comparing energy inputs into a grid versus the capacity of the grid to transport sediment as:

$$P_{i,j}(T_{DS}) = \begin{cases} 1, \text{if } S_i - \Sigma S_{up}/N > 0 \\ 0, \text{if } S_i - \Sigma S_{up}/N \le 0 \end{cases} \quad (12)$$

where ΣS_{up} is the sum of slopes upstream of cell *i*, which is then normalized by the number of upstream cells (N) flowing into a downstream cell *i*. Eq. 12 compares the fluid energy to transport sediment in cell *i* with respect to incoming fluid energy to transport upstream sediment (Mahoney et al., 2018). A cell is considered disconnected to downstream transport if those downstream cells do not have the capacity to entrain further sediment due to flow and energy limitations.

3.2.2. High-frequency turbidity sensing

Fifteen-minute turbidity sensing data were used to investigate the linkage between watershed-scale connectivity and fluvial sediment response. The turbidity data were available from October 2004 to January 2008 and were converted to suspended sediment concentration estimates using linear regressions developed by the USGS (Rasmussen and Gatotho, 2014). Together with streamflow, a complete time-series of suspended sediment load (Q_{SS}, the product of volumetric discharge and sediment concentration) was developed. Thereafter, the 15-min load estimates were integrated to get daily sediment load results to match the temporal frequency of the SWAT and P(C) models. We created linear regressions of watershed-scale P(C) vs daily Q_{SS} for all 'connected days' to assess if the observed sediment transport behavior in the rivers matched the modeled sediment connectivity of the watersheds. A 'connected day' is defined as a day where at least some part of the upland watershed exhibits connectivity (Mahoney et al., 2018), i.e., $P(C) > 0$. Thereafter, we investigated the correlation between P(C) and Q_{SS} for days that were drier than and wetter than the median, respectively, to identify potential breakpoints in when watershed-scale connectivity translates to observed pulses of sediment delivery to streams. The strength of the relationship between P(C) and Q_{SS} was assessed with the Pearson correlation coefficient (ρ).

4. Results

4.1. Runoff and soil moisture modeling

The model simulated and observed flows showed satisfactory agreement for the calibration (2004 to 2005) and validation (2006 to 2007) periods (Fig. S1). The modeled KGE ranged from 0.44 to 0.81 for the calibration period and 0.44 to 0.67 for the validation period. Likewise, the NSE values for calibration and validation periods were also satisfactory and ranged from 0.47 to 0.73 (Table S4). The KGE values for the calibration and validation periods are within acceptable levels reported in the literature and far exceed the minimum threshold (KGE = −0.43) that corresponds to an NSE value of 0 (Knoben et al., 2019). The NSE values are also close to – or greatly exceed – the 0.50 benchmark set as satisfactory by Moriasi et al. (2015). While there is no recognized benchmark for satisfactory p-factor or r-factors, our results fall within general ranges provided in prior studies (Arnold et al., 2012; Abbaspour, 2015). The best performing models are those of Mill Creek and Indian Creek, which are the most highly urbanized basins and have the most immediate streamflow reaction in response to rainfall. The high degree of impervious area in the urban basins simplifies some of the hydrologic processes as urban landscapes generate more runoff and do not have to resolve baseflow and soil moisture conditions to the same degree of accuracy as is required by rural basins to achieve similar model performance. Lastly, we performed a split-sample calibration scheme – a constraint imposed by the SWAT software – whereas a k-fold cross-validation has the potential to generate more robust results (Shen et al., 2022). These limitations notwithstanding, the SWAT models were able to satisfactorily resolve the physics of water flow, particularly the

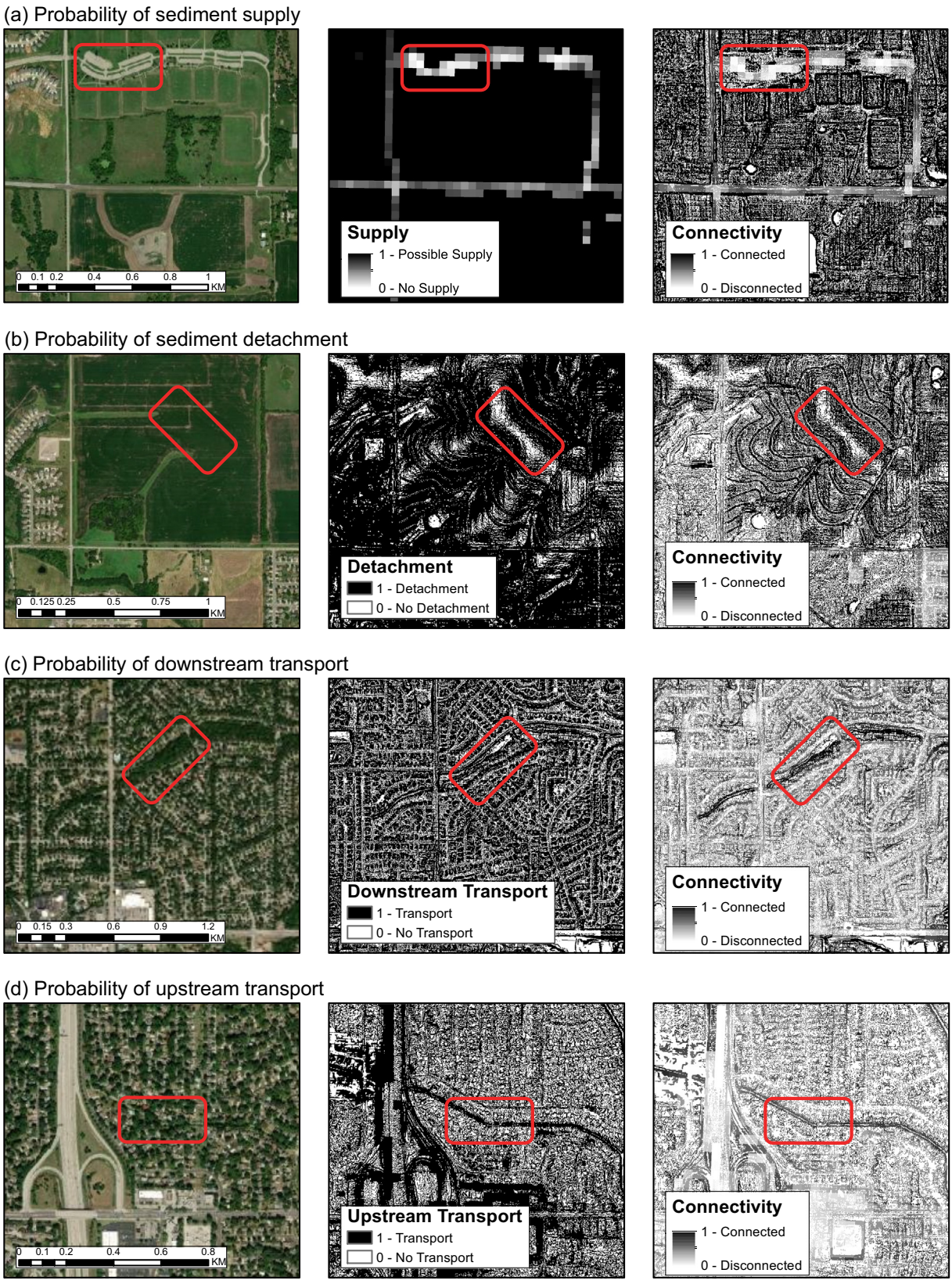

Fig. 3. The impact of (a) sediment supply, (b) sediment detachment, (c) downstream transport, and (d) upstream transport on overall Probability of Connectivity. (a) Roads and parking lots limit the sediment source near a soccer field in rural Blue River. (b) Portions of an agricultural ridge with insufficient runoff to induce detachment in Kill Creek. (c) Steep roadside drainages where downstream sediment transport is channelized in Mill Creek. (d) Urban drainage networks in Indian Creek generate sufficient upstream inputs into channelized flow paths to sustain sediment transport capacity.

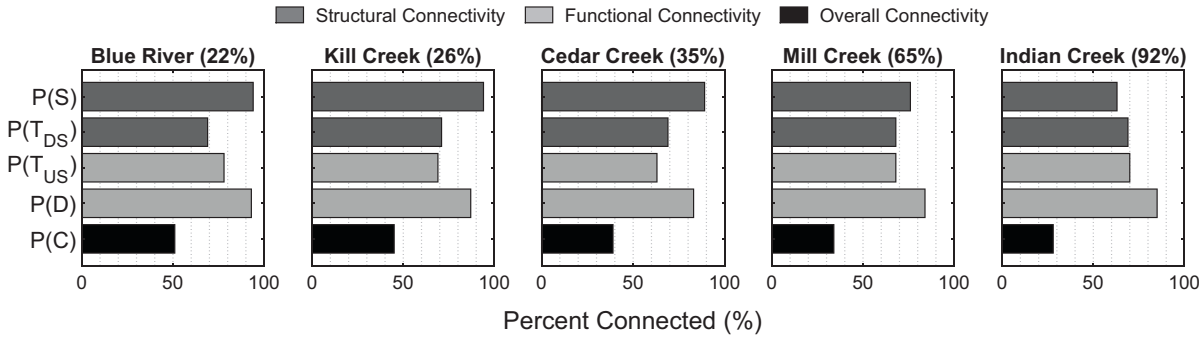

Fig. 4. Basin-scale connectivity probabilities for the wettest (most connected) day for each watershed. Structural connectivity indicators, those that do not change from day-to-day, are supply P(S) and downstream transport P(T_{DS}). Functional connectivity indicators, those that depend on runoff and soil moisture, are detachment P(T_D) and upstream transport P(T_{US}). The percent urban land cover for each watershed is indicated in the title of each subplot.

spatially explicit runoff depths and soil moisture contents, which are crucial inputs for the sediment connectivity model.

4.2. Dynamic connectivity modeling

4.2.1. Evaluating probabilistic controls of connectivity

Over the four-year period, our watershed-scale model predicted the potential for connectivity on 23.9 ± 4.2 % of days. To validate sediment connectivity model outputs and how they are impacted by urbanization, we first visually assessed how each probability in Eq. (6) represented erosion mechanisms, such as sediment supply, detachment, transport, and overall connectivity (Fig. 3). Regarding supply P(S), our model predicts that the presence of impervious surfaces, such as parking lots and roadways, can be a limiting control of connectivity as these surfaces remove sediment supply from the sediment cascade and function as a source of disconnectivity (Fig. 3a). With respect to detachment P(D), as an example, our model identifies low-gradient ridges in an agricultural field that do not generate sufficient shear for sediment entrainment (Fig. 3b). Regarding downstream transport P(T_{DS}), water routing through roadside ditches often provides efficient transport pathways for downstream sediment connection (Fig. 3c). Lastly, upstream transport P(T_{US}) is shown to be an important factor when the upstream drainage area to a grid cell can generate large amounts of runoff through high soil moisture conditions, as is the case in channelized urban drainage systems (Fig. 3d). There was extensive evidence of these supply, detachment, and transport processes and twenty additional examples across all basins are presented in the Supplemental Material (Figs. S2 to S6). Taken together, these visual observations indicate that the sediment connectivity model satisfactorily captures well-established erosion mechanisms, including supply, detachment, upstream energy inputs, and downstream transport.

Next, we investigated the relative importance of each probability component to a basin's overall sediment connectivity (Fig. 4). We select the wettest day of the study period for each basin to aid in comparison, including Blue River (May 7, 2007), Kill Creek (June 6, 2005), Cedar Creek (May 6, 2007), Mill Creek (Aug 26, 2005), and Indian Creek (May 7, 2007). The first observation is that the rural watersheds (Blue River, Kill Creek, and Cedar Creek) have a higher overall P(C) on their wettest days compared to the urban watersheds (Mill Creek and Indian Creek). Regarding the structural probability indicators, i.e., those that do not change in response to hydrology, the probability for downstream transport P(T_{DS}) is approximately the same for all five watersheds, potentially because the mean slope in all basins is approximately 3.7°, whereas the probability of supply P(S) shows a substantial gradient of decrease from rural to urban land use. Results show that the direct impact of urbanization on connectivity is the removal of the spatial extent of available sediment supply, thus putting an 'upper limit' on the amount of a watershed that may be connected during large hydrologic events. Regarding the functional connectivity indicators, i.e., those that depend on runoff depth and soil moisture, there does not appear to be any systematic change in the watershed-scale probability of upstream transport P(T_{US}) and/or the probability of detachment P(D) with percent urban land use. The interplay of the static and dynamic connectivity indicators is highly variable in space (and time for the case of dynamic indicators), and as such there are zones where supply, detachment, and transport are all possible, thus promoting connectivity, and other zones where one (or more) of these indicators is not possible, thus promoting disconnectivity.

The modeled time series of connectivity indicators highlights the importance of dynamic sediment detachment P(D) and upstream transport P(T_{US}) towards overall sediment connectivity (Fig. 5). Recall that in our multiplicative formulation of connectivity (Eq. 6), if a single probability indicator is equal to "0", suggesting some limiting disconnectivity, then the overall probability of connectivity P(C) likewise equals "0". Given this, it is evident from the time series that overall connectivity P(C) is most closely associated with the probability for detachment P(D), which exerts primary control over connectivity. There exist many instances where the probability of upstream transport P(T_{US}) is possible, but overall connectivity does not occur. The reason for this is that while the upstream drainage may be capable of generating overland flow to the cell of interest, the flow inputs do not necessarily exceed the critical shear required for detachment thus preventing connectivity. The probabilities of supply P(S) and downstream transport P(T_{DS}) are static and depend only on topography, morphology, and land cover, which are factors that remain relatively constant over the duration of the study. Our results show that the probability of supply P(S) and downstream transport P(T_{DS}) put a static upper limit on connectivity through either source or transport limitation, respectively. The probabilities of detachment P(D) and upstream transport P(T_{US}) are dynamic and result in grid cells and pathways turning "on" or "off" depending on hydrologic conditions.

4.2.2. Evaluating land use impacts on watershed-scale connectivity

Sediment connectivity was spatially distributed across all watersheds and, on the wettest day for each basin, the urban watersheds were systematically less connected than the rural watersheds (Fig. 6). From least-urban to most-urban, the percent of each watershed connected on its wettest day was 51 %, 45 %, 38 %, 34 %, and 28 %. The defining difference between urban and rural watersheds for sediment connectivity is the degree of impervious land cover (Fig. 7a). Impervious surfaces cover 5.7 % of the most-rural basin compared to 37.4 % of the most-urban basin. Essentially, 37.4 % of the land in the most-urban basin is indefinitely disconnected from the transport cascade. This effect is particularly problematic as all of the watersheds receive the same precipitation inputs, but the sediment available for erosion is concentrated into a much smaller spatial extent in the urban watersheds.

Conversely, when considering all wet days, and not just the single wettest day, our results show that connectivity is more easily established during a typical rain event in the two urban basins than in the rural basins ($p < 0.05$ from Mann-Whitney U Test). This is evident in connectivity results for all wet days where the median P(C), from least-urban to most-

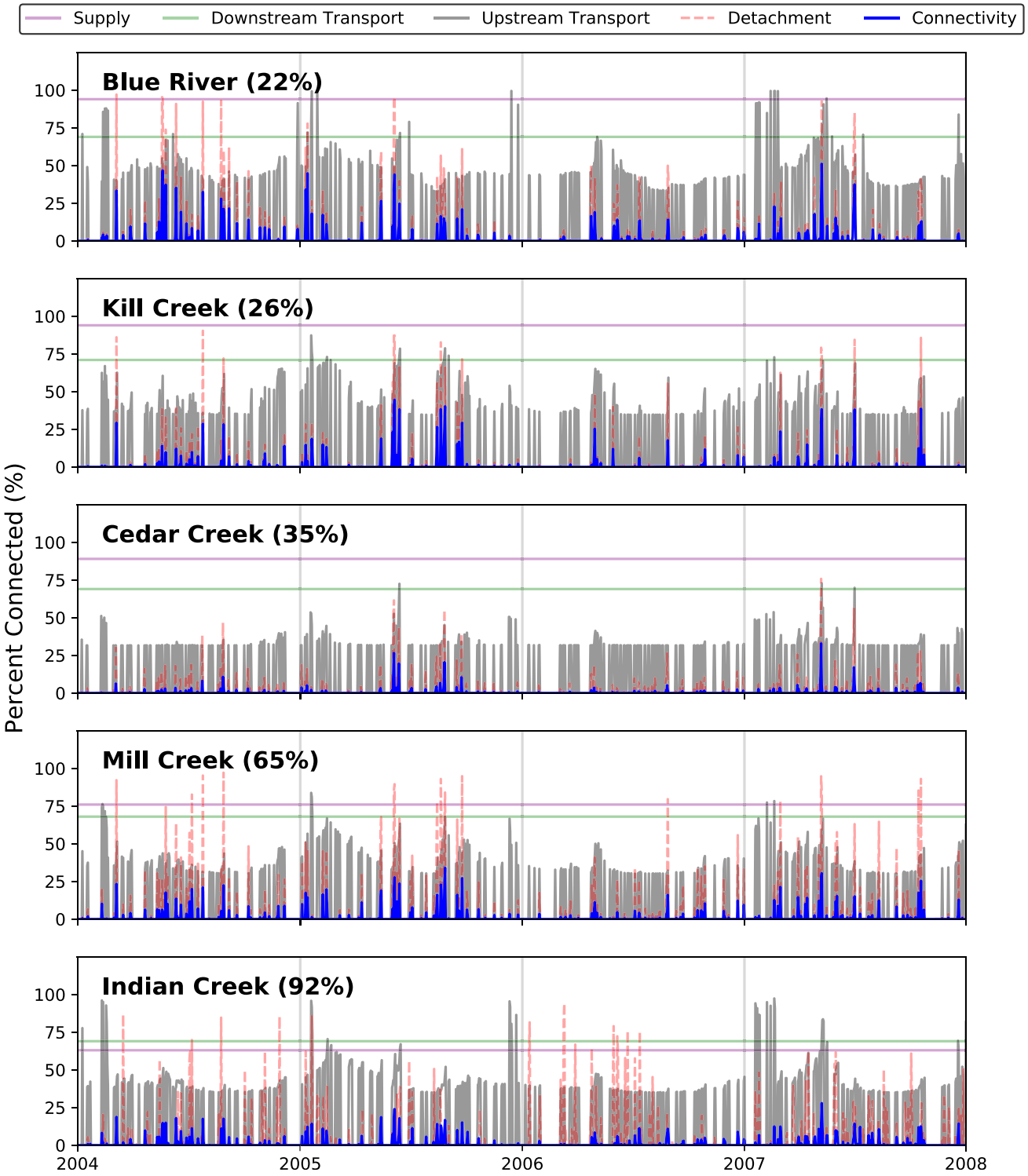

Fig. 5. Modeled time-series of the basin-scale probability of connectivity components, including supply, detachment, upstream transport, and downstream transport. The percent urban land cover for each watershed is indicated in the title of each subplot.

urban, was 0.43 %, 0.18 %, 0.08 %, 1.02 %, and 0.61 % (Fig. 6). The source of this consistent, elevated connectivity was verified through visual assessment to be the extensive drainage network surrounding residential, business, and roadway areas (Fig. 7b). These ephemeral pathways are highly channelized and designed to facilitate the conveyance of water during storm events, leading to their frequent activation as sediment transport pathways. Further, while impervious upstream areas remove the supply of sediment, these same areas generate considerable runoff that provides detachment capability for areas downstream, which may be erodible. Thus, results indicate that while the maximal spatial extent of connectivity is lesser for urban basins, the frequency of connectivity for the typically connected areas is greater.

4.2.3. High frequency turbidity sensing

High frequency turbidity sensing at the pourpoint of each basin was conducted to assess if watershed-scale connectivity influenced the timing and magnitude of the fluvial sediment response (Fig. S7). In general, as the watershed is wetted and sediment becomes connected through

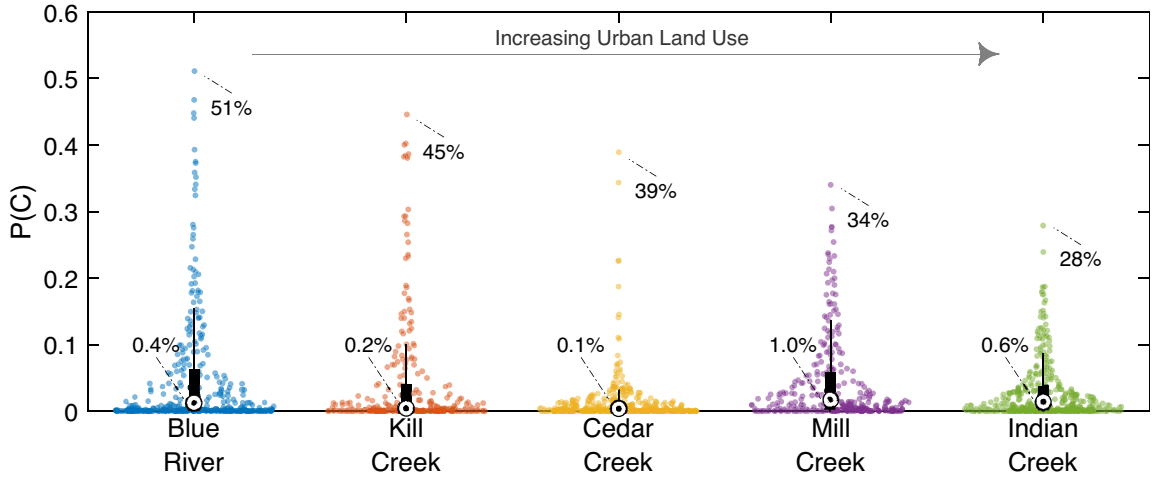

Fig. 6. Combination swarm chart and boxplot of the watershed-scale probability of connectivity P(C), which represents the fraction of a watershed connected to the watershed outlet, for all wet days in the study region. The maximum and median watershed-scale P(C), represented as a percentage, are shown in text next to each swarm chart. Rural basins, such as Blue River, have much greater maximum connectivity than urban basins, like Indian Creek. However, the median connectivity in the urban basins is greater than that of the rural basins.

transport and detachment mechanisms, pulses of sediment loading are observed at the outlet of each watershed. The 23.9 ± 4.2 % of days during the period that have a non-zero extent of watershed-scale functional connectivity account for 85.0 ± 9.5 % of sediment export. Thus, peaks in watershed-scale connectivity generally coincide with large riverine sediment loads. However, there exist days where observed sediment loading and modeled watershed-scale connectivity disagree. Watershed-scale connectivity and in-stream sediment response most frequently differed during periods when low connectivity was predicted but a high sediment load was observed (see early 2006 for all sites in Fig. S7). These results indicate that while watershed-scale connectivity generally correlates with stream loads, there exist other variables that exert an influence on in-stream sediment loads, particularly during drier days.

With the acknowledgement that watershed-scale connectivity and sediment loading do not always agree, we sought to identify potential breakpoints where agreement begins (Fig. 8). In Fig. 8, two linear regressions are shown for the log-transformed values of P(C) and Q_{SS} for each basin: one regression for days that are drier than the median connected day and a second regression for days that are wetter than the median connected day. The drier-than-median day relationship between $\log_{10}[Q_{SS}]$ and $\log_{10}[P(C)]$ is typically very weak (ρ ranges from 0.01 to 0.27; not plotted), suggesting that watershed-scale connectivity and fluvial sediment loading are poorly correlated during low wetness conditions. On the other hand, results show that a linear relationship between $\log_{10}[Q_{SS}]$ and $\log_{10}[P(C)]$ is typically initiated at the median connected day for each basin. For wetter-than-median days, the stream response becomes a function of watershed-scale connectivity with a fairly strong relationship in most basins (ρ ranges from 0.33 to 0.52). Our results indicate that during high-magnitude hydrologic events, P(C) becomes a good predictor for sediment transport because the broad-scale contribution of the collective watershed overrides the effects of the most sensitive, isolated pathways that impart control on sediment transport during smaller events.

5. Discussions

5.1. Urbanization as a limiter and catalyst of watershed-scale sediment transport

Sediment connectivity is governed by the spatial distribution of sediment sources, transfer pathways, and deposition of sediment from source to sink (Fryirs et al., 2007; Poeppl et al., 2020). While urbanization has long been recognized to increase sediment transport, a result largely attributed to more runoff generation and excess shear (Yorke and Herb, 1978; MacKenzie et al., 2022), our study adds additional mechanistic explanations towards a full understanding of watershed-scale sediment export from urban basins. Results from this study indicate that the spread of impervious surfaces limits the available supply of sediment to watershed-scale export during extreme events, which acts as a source of disconnectivity along the sediment cascade. However, urbanization also serves as a "catalyst" for conveying sediment from upstream to downstream locations through the enhancement of runoff, increase in the likelihood of detachment, and frequent wetting of principally connected pathways. Thus, the effects of urbanization on sediment transport are particularly insidious as impervious surfaces indefinitely disconnect sediment in one location from transport while overloading sediment with runoff in a second erodible location.

Connectivity in rural watersheds is limited more by transport than by supply as abundant sediment sources exist for erosion, but adequate runoff for detachment is not always present (Fig. 5). This is consistent with other studies that have applied the probability of connectivity approach in rural and forested watersheds throughout Kentucky, USA (Mahoney et al., 2018; Mahoney et al., 2021). On the other hand, as watersheds undergo urbanization, they transition from transport limitation (as there is now abundant runoff) towards supply limitation (as swaths of land are paved over) (Fryirs et al., 2007). In the most-rural basin, the wettest day of the study period caused 51 % of the watershed to become connected to the watershed outlet. On the other hand, the most-urban basin had a much lower extent of connectivity at just 28 % on its wettest day. These results are largely driven by the impervious land area coverage whereby the most rural basin has 5.7 % impervious area whereas the most urban basin has 37.4 % impervious area. While each component of the probability of connectivity equation, $P(C) = P(S) \cap P(D) \cap P(T)$, acts to reduce overall sediment connectivity, rural basin connectivity is most closely related to the probability of detachment P(D), which sets an upper limit on overall connectivity.

Conversely, urbanization is most closely related to the probability of supply – an important structural property of the watershed – through extensive impervious surfaces that effectively put an upper limit on the P(S) term. Other heavily disturbed watersheds have exhibited similar controls of sediment connectivity. For example, Mahoney et al. (2021) found that the probability of downstream transport – a function of watershed relief (Eq. 12) – most frequently limited sediment connectivity on reclaimed mine surfaces in a catchment in eastern Kentucky. On reclaimed mine surfaces, soil texture disturbance and compaction reduce infiltration rates such that storms frequently produce relatively large runoff volumes compared to the surrounding forestland (Wickham et al., 2007; Warner et al., 2010; Mahoney et al., 2021). Similar to the urban watersheds presented herein,

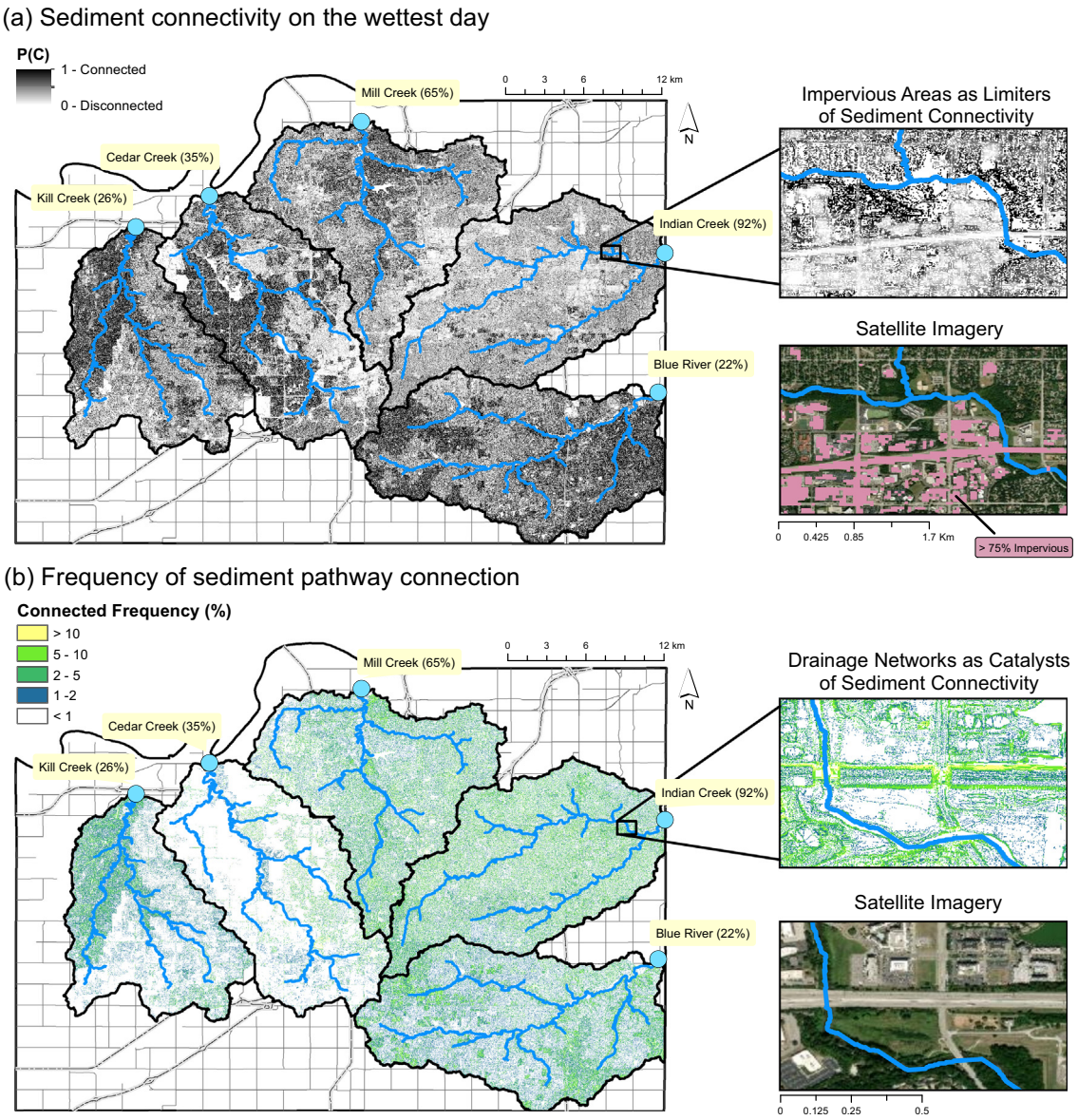

Fig. 7. (a) Probability of sediment connectivity for the wettest days in the study period. As watersheds become more urbanized there is less connectivity overall for the watersheds due to diminished sediment supply with increased urbanization. (b) Frequency of sediment pathway connection. Drainage networks are frequently wetted (>10 % of the days in the period), providing for functional connection to downstream locations. The percent urban land cover for each watershed is indicated in the title of each subplot.

this results in an abundance of fluid energy to detach sediment, and manifests in increased median degrees of connectivity compared to surrounding land uses. In both types of watersheds (i.e., heavily urbanized, reclaimed mine) hydrologic processes no longer functioned as limiters of connectivity, but rather the structural configuration of the watershed – as manifested through the availability of sediment supply or the watershed's relief – did. Taken together, these studies provide evidence of a fundamental shift in the controls of sediment connectivity at the watershed scale as landscape disturbance increases.

However, it is important to note that there exist potential mechanisms related to urbanization that are not captured by our model. For example, when land use is changed from rural to urban and as vegetation is removed, bare soil may become exposed through construction, which maintains sediment supply but drastically reduces critical shear stresses leading to likely detachment. However, these types of construction activities are difficult to capture at the watershed-scale as they exhibit significant spatial and temporal heterogeneity. Further, soon after construction wanes in urban areas, the sediment supply and exposure decline back to low levels as impervious areas are implemented and vegetation is reestablished (Russell, 2021). Likewise, inter- and intra-basin differences in the drainage capability of soils could explain some variation in connectivity results. While the majority of all basins are typified by NRCS hydrologic group B soils (Fig. S8), there are zones of group C and D soils, which have lower infiltration capacity and may promote more runoff generation. Nonetheless, while soil drainage impacts runoff generation, and thus detachment probability, the connectivity results cannot be explained as solely a function of soils and instead also greatly depend on land cover.

5.2. Urbanization focuses sediment transport into fewer, more frequently wetted pathways

While supply limitation hinders the maximal extent of connectivity on the wettest days in urban basins, our results show that for the typical wet day, urban basins exhibit greater baseline connectivity. For example, on the median wet day, an average of 0.82 % of all urban basin lands are

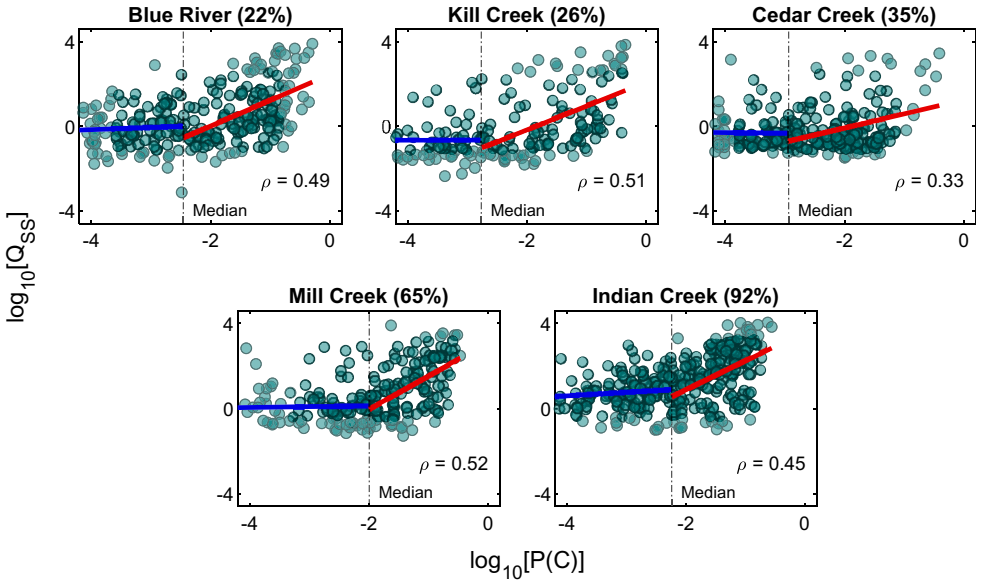

Fig. 8. Modeled sediment connectivity and observed sediment loading (ton/day) for all connected days across the study period. These plots include two linear regressions for below (blue line) and above (red line) the median connected day for each basin (vertical dashed line). Positive correlation (ρ) between connectivity and observed sediment yield are shown for the above-median regression. The percent urban land cover for each watershed is indicated in the title of each subplot.

connected compared to just 0.23 % for rural basins (Fig. 6). Thus, during a common rain event, urban basins exhibit 3.5 times greater connectivity. We attribute this result to the rapid activation of highly sensitive ephemeral pathways in urban basins. These pathways are a result of the construction of drainage networks that aim to route flow through ditches and channels for the efficient removal of water from urban lands (Hu et al., 2001). These drainage networks alter the slope and flow direction of the natural topography and increase the capacity for fluid shear stress to produce hydrologic connectivity, resulting in more concentrated flow pathways for sediment transport (Llena et al., 2019; Mahoney et al., 2018; Zarnaghsh and Husic, 2021; Batista et al., 2022). It is important to note that the process of intense agriculture can also create channelized pathways, such as in areas where native vegetation is removed and replaced with row crops (Bracken et al., 2015; Persichillo et al., 2017), but for our study area we see this phenomenon most prominently in urban basins.

Recent work has noted that the most sensitive sediment transport pathways in watersheds disproportionately contribute to large amount of sediment yield (Mahoney et al., 2020b). To this end, prior modeling work in our study area estimated that as much as 37 ± 4 % of total erosion was constrained to as little as 5 ± 1 % of the study drainage area (Michalek et al., 2021), highlighting the need to identify areas that are frequently connected. Batista et al. (2022) also found that higher sediment yields were calculated when roads acted as hydraulic conveyor belts between upland sediment patches and downstream river networks. In this study, we find that – irrespective of land use – the fluvial sediment response only begins to correlate with basin-scale sediment connectivity once the watershed exceeds a certain threshold for connectedness, that is the 'median connected day' (Fig. 8). For half of all connected days, there is essentially no correlation between watershed-scale connectivity and in-stream sediment loading ($\rho < 0.27$). However, once the median connectedness threshold is exceeded, connectivity and fluvial sediment loading begin to agree (ρ between 0.33 and 0.52). While recent work has indicated that sediment connectivity alone cannot predict sediment transport (Mahoney et al., 2018; Mahoney et al., 2020b), our work indicates that there may be thresholds when the two become more closely linked. These breakpoints in the (de)coupling of stream and watershed response may be indicative of a shift from functional to structural connectivity (Borselli et al., 2008; Mahoney et al., 2020b). Thus, results suggest that local heterogeneities and topographic disconnectivities dominate the sediment load during the drier half of connected days, whereas the watershed-scale response prevails given enough hydrologic forcing from large events, and that frequency of pathway wetting is a critical component of sediment delivery to streams.

5.3. Probabilistic modeling to inform best practices and future directions

Nearly all stakeholders who are aware of connectivity-related linkages use that knowledge to influence their management (Smetanová et al., 2018); however, due to a lack of data availability and practical methodology, less than one-quarter of stakeholders have this awareness. Thus, potential exists for functional connectivity models, such as P(C), to serve as a land management tool for soil loss mitigation (Mahoney et al., 2018, 2020a, 2020b). Process-based functional connectivity models have the advantage of simulating dynamic behavior that may change through space and time, whereas structural connectivity models are static through time. Thus, the P(C) model can be used for cost-effective insight into areas where sediment is available, easily detachable, and where transport pathways exist. For example, in our urban catchments the P(C) model can be used as a tool to identify urban areas that are at risk, which may benefit from the installation of erosion control structures to mitigate channel erosion. Additionally, in erosion-prone agriculture fields, the P(C) model can be used to identify fields to apply sediment control measures such as vegetation buffers to decrease sediment input from the arable land to water bodies (Batista et al., 2022).

The next steps for the probability of connectivity model application to our watershed would be to incorporate fine-scale mechanistic transport modeling to resolve disagreements between watershed-scale connectivity and fluvial sediment loading. As noted in our results and prior studies (Mahoney et al., 2018, 2020b), watershed-scale connectivity is not always a great predictor of sediment transport. This is in contrast to Vigiak et al. (2012) where the authors of that study find that watershed connectivity is a significant predictor of sediment flux. Our results provide context to this apparent disagreement in the literature. First, the timescale of observation matters, where Vigiak et al. (2012) studied sediment connectivity at annual timescales while Mahoney et al. (2020b) assed it at daily timescales. If one looks at connectivity during only the most extreme annual events over the course of decades, our results indicate that there is agreement of connectivity with in-stream loading when a threshold of connectedness is exceeded. In these instances, long-term sediment connectivity patterns are controlled by structural connectivity (Fryirs, 2013). However, at the timescale of events that occur dozens of times within a year, smaller

heterogeneities within a watershed exert more influence than basin-scale processes, suggesting that functional – rather than structural – connectivity prevails as a driver in these instances. Hence, to predict sediment flux, sediment connectivity modeling needs to be coupled with sediment erosion and routing formulae (Mahoney et al., 2020b) because sediment connectivity and transport encompasses both structural and functional connectivity (Fryirs, 2013; Bracken et al., 2015; Mahoney et al., 2020b).

While the P(C) model shows considerable utility, there are some limitations worth discussing. First, in an effort to simplify sediment transport processes and avoid explicitly simulating the sediment continuity equation for each pixel in the watershed (an endeavor that would be computationally and epistemologically prohibitive), the P(C) approach does not explicitly route sediment but rather looks at *potential* connectivity based on runoff depths and soil moisture. Second, we do not consider the probability of buffers in Eq. (7). Buffers, such as floodplains, exist in all watersheds to varying degrees. We do not have evidence that buffers are more prominent in one watershed versus another, thus the exclusion of buffers should not alter our overall results considerably. Further, in Mahoney et al. (2018), the probability of buffers was the least influential of all parameters in Eq. (7). Third, we do not consider the probability of non-hydrologic detachment, such as mass-wasting events, construction activities, and tillage. These phenomena are highly isolated in both space and time and difficult to constrain with a watershed-scale assessment that primarily focuses on non-point source processes. The resolution of our impervious dataset is 30-m by 30-m, which could be improved further to reflect the 2-m by 2-m DEM that is used for topographic assessment as sediment supply in urban settings can vary drastically from construction sites to open fields (Russell et al., 2018; Russell, 2021). Despite these limitations, our modeling effort is robust, provides results that are corroborated by previous literature, and makes new insights into the effects of land use on sediment connectivity.

6. Conclusions

The overarching goal of this study was to assess how urbanization impacts sediment connectivity at the watershed-scale. Model results suggest impervious surface cover plays a crucial role in determining the spatial extent and degree of watershed-scale sediment connectivity. In urban basins, maximal sediment connectivity is relatively low due to the proliferation of paved surfaces. On the other hand, these impervious surfaces generate considerable runoff that is conveyed to potentially erodible downstream locations. For this reason, sensitive ephemeral pathways in urban basins are wetted 3.5 times more frequently than the equivalent pathways in rural basins. Our results suggest that the typical (or median) connected day serves as a breakpoint for when watershed-scale connectivity begins to influence riverine sediment loading. The P(C) modeling approach can be used as a tool to illuminate how watershed configuration dictates where sediment transport may occur, such as in erosion and connectivity hotspots in urban drainage systems or agriculture fields.

CRediT authorship contribution statement

Isaac McVey: Conceptualization, Investigation, Methodology, Software, Data curation, Formal analysis, Visualization, Writing – original draft, Writing – review & editing. **Alexander Michalek:** Methodology, Software, Data curation, Formal analysis, Writing – review & editing. **Tyler Mahoney:** Methodology, Software, Data curation, Formal analysis, Writing – review & editing. **Admin Husic:** Conceptualization, Investigation, Methodology, Software, Data curation, Formal analysis, Visualization, Writing – original draft, Writing – review & editing.

Data availability

Data will be made available on request.

Declaration of competing interest

The authors declare that they have no known competing financial interests or personal relationships that could have appeared to influence the work reported in this paper.

Acknowledgments

The authors thank the associate editor and three anonymous reviewers for their feedback on this manuscript, which has improved its quality. We would like to recognize the Department of Civil, Environmental, and Architectural Engineering and the Department of Geography and Atmospheric Sciences at University of Kansas for providing partial funding to the student authors of this manuscript. We would like to also acknowledge Johnson County AIMS for providing us with the high-resolution LiDAR data used in this study. Lastly, we obtained solar radiation data from the NASA Langley Research Center POWER Project, which is funded through the NASA Earth Science Directorate Applied Science Program. The authors declare no competing interests.

Appendix A. Supplementary data

Supplementary data to this article can be found online at https://doi.org/10.1016/j.scitotenv.2023.165093.

References

Abbaspour, K.C., Yang, J., Maximov, I., Siber, R., Bogner, K., Mieleitner, J., Zobrist, J., Srinivasan, R., 2007. Modelling hydrology and water quality in the pre-alpine/alpine Thur watershed using SWAT. J. Hydrol. 333 (2), 413–430. https://doi.org/10.1016/j.jhydrol.2006.09.014.

Abbaspour, Karim C., 2015. SWAT-CUP: SWAT Calibration and Uncertainty Programs—A User Manual. Eawag, Dübendorf, Switzerland, pp. 16–70.

AIMS, 2020. Johnson County Automated Information Mapping System. https://maps.jocogov.org/ims/. (Accessed 24 November 2020).

Alberts, E.E., Nearing, M.A., Weltz, M.A., Risse, L.M., Pierson, F.B., Zhang, X.C., Laflen, J.M., Simanton, J.R., 1995. Chapter 7 soil component. In: Flanagan, D.C., Nearing, M.A. (Eds.), USDA. Water erosion and Prediction Project Hillslope Profile and Watershed Model Documentation. NSERL Report No. 10 USDA-ARS National Soil Erosion Research Laboratory, West Lafayette, Indiana 47907.

Arnold, J.G., Srinivasan, R., Muttiah, R.S., Williams, J.R., 1998. Large area hydrologic modeling and assessment part I: model development1. JAWRA Journal of the American Water Resources Association 34 (1), 73–89. https://doi.org/10.1111/j.1752-1688.1998.tb05961.x.

Arnold, J.G., Moriasi, D.N., Gassman, P.W., Abbaspour, K.C., White, M.J., Srinivasan, R., Santhi, C., Harmel, R.D., van Griensven, A., Van Liew, M.W., Kannan, N., Jha, M.K., 2012. SWAT: model use, calibration, and validation. Trans. ASABE 55 (4), 1491–1508. https://doi.org/10.13031/2013.42256.

Baartman, J.E., Nunes, J.P., Masselink, R., Darboux, F., Bielders, C., Degré, A., Cantreul, V., Cerdan, O., Grangeon, T., Fiener, P., Wilken, F., Schindewolf, M., Wainwright, J., 2020. What do models tell us about water and sediment connectivity? Geomorphology 367, 107300. https://doi.org/10.1016/j.geomorph.2020.107300.

Baldan, D., Cunillera-Montcusí, D., Funk, A., Hein, T., 2022. Introducing 'riverconn': an R package to assess river connectivity indices. Environ. Model Softw. 156, 105470. https://doi.org/10.1016/j.envsoft.2022.105470.

Batista, P.V.G., Fiener, P., Scheper, S., Alewell, C., 2022. A conceptual-model-based sediment connectivity assessment for patchy agricultural catchments. Hydrol. Earth Syst. Sci. 26 (14), 3753–3770. https://doi.org/10.5194/hess-26-3753-2022.

Bettencourt, L., Clarens, A., Das, S., Fitzgerald, G., Irwin, E., Pataki, D., et al., 2018. Sustainable Urban Systems: Articulating a Long-Term Convergence Research Agenda. Retrieved from, Sustainable Urban Systems. https://www.nsf.gov/ere/ereweb/ac-ere/sustainable-urban-systems.pdf.

Borrelli, P., Robinson, D.A., Panagos, P., Lugato, E., Yang, J.E., Alewell, C., Wuepper, D., Montanarella, L., Ballabio, C., 2020. Land use and climate change impacts on global soil erosion by water (2015-2070). Proc. Natl. Acad. Sci. 117 (36), 21994–22001.

Borselli, L., Cassi, P., Torri, D., 2008. Prolegomena to sediment and flow connectivity in the landscape: a GIS and field numerical assessment. CATENA 75 (3), 268–277. https://doi.org/10.1016/j.catena.2008.07.006.

Bracken, L.J., Turnbull, L., Wainwright, J., Bogaart, P., 2015. Sediment connectivity: a framework for understanding sediment transfer at multiple scales. Earth Surf. Process. Landf. 40 (2), 177–188.

Clark, M.P., Vogel, R.M., Lamontagne, J.R., Mizukami, N., Knoben, W.J.M., Tang, G., Gharari, S., Freer, J.E., Whitfield, P.H., Shook, K.R., Papalexiou, S.M., 2021. The abuse of popular performance metrics in hydrologic modeling. Water Resour. Res. 57 (9). https://doi.org/10.1029/2020WR029001.

Crema, S., Cavalli, M., 2018. SedInConnect: a stand-alone, free and open source tool for the assessment of sediment connectivity. Comput. Geosci. 111, 39–45. https://doi.org/10.1016/j.cageo.2017.10.009.

Ferreira, C.S.S., Walsh, R.P.D., Kalantari, Z., Ferreira, A.J.D., 2020. Impact of land-use changes on spatiotemporal suspended sediment dynamics within a Peri-urban catchment. Water 12 (3), 665. https://doi.org/10.3390/w12030665.

Fryirs, K., 2013. (dis)connectivity in catchment sediment cascades: a fresh look at the sediment delivery problem. Earth Surf. Process. Landf. 38 (1), 30–46. https://doi.org/10.1002/esp.3242.

Fryirs, K.A., Brierley, G.J., Preston, N.J., Kasai, M., 2007. Buffers, barriers and blankets: the (dis)connectivity of catchment-scale sediment cascades. CATENA 70 (1), 49–67. https://doi.org/10.1016/j.catena.2006.07.007.

Heckmann, T., Cavalli, M., Cerdan, O., Foerster, S., Javaux, M., Lode, E., Smetanová, A., Vericat, D., Brardinoni, F., 2018. Indices of sediment connectivity: opportunities, challenges and limitations. Earth Sci. Rev. 187, 77–108. https://doi.org/10.1016/j.earscirev.2018.08.004.

Hu, S., Zhi-mao, G., Jun-ping, Y., 2001. The impacts of urbanization on soil erosion in the loess plateau region. J. Geogr. Sci. 11 (3), 282–290. https://doi.org/10.1007/BF02892311.

Husic, A., Michalek, A., 2022. Structural hillslope connectivity is driven by tectonics more than climate and modulates hydrologic extremes and benefits. Geophys. Res. Lett. 49 (15). https://doi.org/10.1029/2022GL099898.

Knoben, W.J.M., Freer, J.E., Woods, R.A., 2019. Technical note: Inherent benchmark or not? Comparing Nash–Sutcliffe and Kling–Gupta efficiency scores. Hydrol. Earth Syst. Sci. 23 (10), 4323–4331. https://doi.org/10.5194/hess-23-4323-2019.

Kroese, Stenfert J., Batista, P.V.G., Jacobs, S.R., Breuer, L., Quinton, J.N., Rufino, M.C., 2020. Agricultural land is the main source of stream sediments after conversion of an African montane forest. Sci. Rep. 10 (1). https://doi.org/10.1038/s41598-020-71924-9 Article 1.

Llena, M., Vericat, D., Cavalli, M., Crema, S., Smith, M.W., 2019. The effects of land use and topographic changes on sediment connectivity in mountain catchments. Sci. Total Environ. 660, 899–912. https://doi.org/10.1016/j.scitotenv.2018.12.479.

MacKenzie, K.M., Singh, K., Binns, A.D., Whiteley, H.R., Gharabaghi, B., 2022. Effects of urbanization on stream flow, sediment, and phosphorous regime. J. Hydrol. 612, 128283. https://doi.org/10.1016/j.jhydrol.2022.128283.

Mahoney, D., Fox, J., Al-Aamery, N., Clare, E., 2020a. Integrating connectivity theory within watershed modelling part I: model formulation and investigating the timing of sediment connectivity. Sci. Total Environ. 740, 140385. https://doi.org/10.1016/j.scitotenv.2020.140385.

Mahoney, D., Blandford, B., Fox, J., 2021. Coupling the probability of connectivity and RUSLE reveals pathways of sediment transport and soil loss rates for forest and reclaimed mine landscapes. J. Hydrol. 594 (2021), 125963.

Mahoney, D.T., Fox, J.F., Al Aamery, N., 2018. Watershed erosion modeling using the probability of sediment connectivity in a gently rolling system. J. Hydrol. 561, 862–883. https://doi.org/10.1016/j.jhydrol.2018.04.034.

Mahoney, D.T., Fox, J., Al-Aamery, N., Clare, E., 2020b. Integrating connectivity theory within watershed modelling part II: application and evaluating structural and functional connectivity. Sci. Total Environ. 740, 140386. https://doi.org/10.1016/j.scitotenv.2020.140386.

Michalek, A., Zarnaghsh, A., Husic, A., 2021. Modeling linkages between erosion and connectivity in an urbanizing landscape. Sci. Total Environ. 764, 144255. https://doi.org/10.1016/j.scitotenv.2020.144255.

Moriasi, D.N., Arnold, J.G., Van Liew, M.W., Bingner, R.L., Harmel, R.D., Veith, T.L., 2015. Hydrologic and water quality models: performance measures and evaluation criteria. Trans. ASABE 58 (6), 1763–1785. https://doi.org/10.13031/trans.58.10715.

Natural Resource Conservation Service NRCS, 1972. Hydrology. National Engineering Handbook, Sec. 4, U.S. Department of Agriculture, Washington, D.C.

NLCD, 2004. NLCD. Multi-Resolution Land Characteristics (MRLC) Consortium. https://www.mrlc.gov/.2004.

NLCD, 2006. NLCD. Multi-Resolution Land Characteristics (MRLC) Consortium. https://www.mrlc.gov/.2006.

Noe, G.B., Cashman, M.J., Skalak, K., Gellis, A., Hopkins, K.G., Moyer, D., Webber, J., Benthem, A., Maloney, K., Brakebill, J., Sekellick, A., Langland, M., Zhang, Q., Shenk, G., Keisman, J., Hupp, C., 2020. Sediment dynamics and implications for management: state of the science from long-term research in the Chesapeake Bay watershed, USA. WIREs Water 7 (4), e1454. https://doi.org/10.1002/wat2.1454.

Percich, A., Husic, A., Ketterer, M.E., 2022. Plutonium isotopes: an effective tool for fluvial sediment sourcing in urbanized catchments. Geophys. Res. Lett. 49 (2). https://doi.org/10.1029/2021GL094497.

Persichillo, M.G., Bordoni, M., Meisina, C., 2017. The role of land use changes in the distribution of shallow landslides. Sci. Total Environ. 574, 924–937.

Persichillo, M.G., Bordoni, M., Cavalli, M., Crema, S., Meisina, C., 2018. The role of human activities on sediment connectivity of shallow landslides. CATENA 160, 261–274. https://doi.org/10.1016/j.catena.2017.09.025.

Poeppl, R.E., Fryirs, K.A., Tunnicliffe, J., Brierley, G.J., 2020. Managing sediment (dis)connectivity in fluvial systems. Sci. Total Environ. 736, 139627. https://doi.org/10.1016/j.scitotenv.2020.139627.

Rasmussen, T.J., Gatotho, J., 2014. Water-quality variability and constituent transport and processes in streams of Johnson County, Kansas, using continuous monitoring and regression models. 2003–11: U.S. Geological Survey Scientific Investigations Report 2013–5221 , p. 53.. https://doi.org/10.3133/sir20135221.

Russell, K., 2021. Potential sediment supply fluxes associated with greenfield residential construction. Anthropocene 35, 100300. https://doi.org/10.1016/j.ancene.2021.100300.

Russell, K.L., Vietz, G.J., Fletcher, T.D., 2018. Urban catchment runoff increases bedload sediment yield and particle size in stream channels. Anthropocene 23, 53–66. https://doi.org/10.1016/j.ancene.2018.09.001.

Shen, H., Tolson, B.A., Mai, J., 2022. Time to update the split-sample approach in hydrological model calibration. Water Resour. Res. 58 (3). https://doi.org/10.1029/2021wr031523.

Smetanová, A., Paton, E.N., Maynard, C., Tindale, S., Fernández-Getino, A.P., Marqéus Pérez, M.J., Bracken, L., Le Bissonnais, Y., Keesstra, S.D., 2018. Stakeholders' perception of the relevance of water and sediment connectivity in water and land management. Land Degrad. Dev. 29 (6), 1833–1844. https://doi.org/10.1002/ldr.2934.

Sparks, A.H., 2018. Nasapower: a NASA POWER global meteorology, surface solar energy and climatology data client for R. The Journal of Open Source Software 3 (30), 1035. https://doi.org/10.21105/joss.01035.

StormWatch, 2020. Johnson County, Kansas StormWATCH. https://www.stormwatch.com/home.php.2020.

Torri, D., Poesen, J., 2014. A review of topographic threshold conditions for gully head development in different environments. Earth Sci. Rev. 130, 73–85. https://doi.org/10.1016/j.earscirev.2013.12.00.

USCB, 2007. TIGER/Line Shapefiles. https://www.census.gov/geographies/mapping-files/time-series/geo/tiger-line-file.html. (Accessed 1 January 2021).

USCB, 2020. 2020 Census Results. https://www.census.gov/programs-surveys/decennial-census/decade/2020/2020-census-results.html. (Accessed 1 January 2021).

USDA, 2021. USDA web soil survey. https://www.nrcs.usda.gov/wps/portal/nrcs/main/soils/survey/. (Accessed 8 November 2021).

USDA, 2022. USDA web soil survey. https://www.nrcs.usda.gov/wps/portal/nrcs/main/soils/survey/. (Accessed 7 September 2022).

USGS, 2018. USGS. National Water Information System Data Available on the World Wide Web (USGS Water Data for the Nation). https://waterdata.usgs.gov/nwis/ (2018), Accessed 20th Sep 2018.

Vandaele, K., 1993. Assessment of factors affecting ephemeral gully erosion in cultivated catchments of the Belgian Loam Belt. In: S. Wicherek (editor), Farm Land Erosion in Temperate.

Vigiak, O., Borselli, L., Newham, L.T.H., McInnes, J., Roberts, A.M., 2012. Comparison of conceptual landscape metrics to define hillslope-scale sediment delivery ratio. Geomorphology 138 (1), 74–88. https://doi.org/10.1016/j.geomorph.2011.08.026.

Warner, R.C., Agouridis, C.T., Vingralek, P.T., Fogle, A.W., 2010. Reclaimed Mineland curve number response to temporal distribution of rainfall. JAWRA Journal of the American Water Resources Association 46 (4), 724–732. https://doi.org/10.1111/j.1752-1688.2010.00444.x.

Wellen, C., Kamran-Disfani, A.-R., Arhonditsis, G.B., 2015. Evaluation of the current state of distributed watershed nutrient water quality modeling. Environ. Sci. Technol. 49 (6), 3278–3290. https://doi.org/10.1021/es5049557.

Wickham, J., Stehman, S.V., Sorenson, D.G., Gass, L., Dewitz, J.A., 2021. Thematic accuracy assessment of the NLCD 2016 land cover for the conterminous United States. Remote Sens. Environ. 257, 112357. https://doi.org/10.1016/j.rse.2021.112357.

Wickham, J.D., Riitters, K.H., Wade, T.G., Coan, M., Homer, C., 2007. The effect of Appalachian mountaintop mining on interior forest. Landsc. Ecol. 22 (2), 179–187. https://doi.org/10.1007/s10980-006-9040-z.

Wood, P., Armitage, P., 1997. Biological effects of fine sediment in the lotic environment. Environ. Manag. 21 (2), 203–217. https://doi.org/10.1007/s002679900019.

Yorke, T.H., Herb, W.J., 1978. Effects of Urbanization on Streamflow and Sediment Transport in the Rock Creek and Anacostia River Basins, Montgomery County, Maryland. , pp. 74–1962 https://doi.org/10.3133/pp1003.

Zarnaghsh, A., Husic, A., 2021. Degree of anthropogenic land disturbance controls fluvial sediment hysteresis. Environ. Sci. Technol. 55 (20), 13737–13748. https://doi.org/10.1021/acs.est.1c00740.

Zhang, C., Huang, Y., Javed, A., Arhonditsis, G.B., 2019. An ensemble modeling framework to study the effects of climate change on the trophic state of shallow reservoirs. Sci. Total Environ. 697, 134078. https://doi.org/10.1016/j.scitotenv.2019.134078.